



INHIBITION OF CARBOXYPEPTIDASE A BY N-(4-*t*-BUTYLBENZOYL)-2-HYDROXY-1-NAPHTHALDEHYDE HYDRAZONE

Christopher M. Lanthier,^a Michael A. Parniak^b and Gary I. Dmitrienko^{a*}

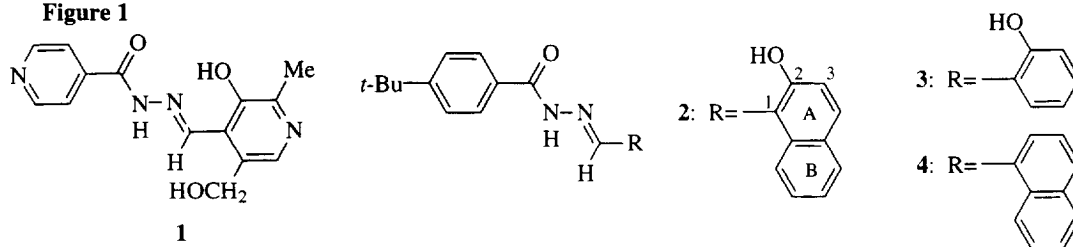
^aDepartment of Chemistry, University of Waterloo, Waterloo, Ontario, Canada N2L 3G1

^bLady Davis Institute for Medical Research, Sir Mortimer B. Davis-Jewish General Hospital,
3755 Cote Ste. Catherine Road, Montreal, Quebec, Canada H3T 1E2

Abstract : N-(4-*t*-Butylbenzoyl)-2-hydroxy-1-naphthaldehyde hydrazone (**2**), which is a potent inhibitor of HIV-1 reverse transcriptase, was found to inhibit carboxypeptidase A in a mixed uncompetitive-competitive mode. Molecular modeling studies suggest that **2** may inhibit CPA by binding to the S₁ and S₂ subsites of free CPA as well as to the CPA-phenylalanine binary enzyme-product complex. © 1997 Elsevier Science Ltd.

N-Acylhydrazones (NAH's) have been studied as potential therapeutic agents in a number of pharmaceutical contexts. For example PIH (**1**) and related compounds have been shown to be potent chelators for Fe³⁺ and, as such, have been examined as potential medicinal agents for the treatment of iron overload in patients suffering from thalassemia with somewhat promising results.¹ Other reports indicate that NAH's can exhibit antimalarial properties putatively through the inhibition of the cysteine protease falcipaine,² as well as antibiotic and antifungal activities through an unknown mechanism.³ Of particular interest is the observation that the toxicity usually associated with non-specific metal binding agents is much less pronounced with the NAH's, some of which have been employed in clinical trials.

Figure 1



Recent studies in these laboratories have revealed that certain NAH's are specific inhibitors of both the RNA-dependent DNA polymerase and the RNase H activities of HIV-1 reverse transcriptase (RT).⁴ RNases H from *E. coli* and from *Thermus thermophilus* are also susceptible to inhibition by NAH's, but the structure activity relationship amongst the NAH's observed for inhibition of the bacterial enzymes differs significantly from that observed for the retroviral enzyme.⁵

The possibility that NAH's might also be relatively nontoxic inhibitors of divalent metal ion dependent proteolytic enzymes prompted us to carry out preliminary experiments concerning the interaction of NAH's with carboxypeptidase A (CPA) and angiotensin converting enzyme (ACE), both of which utilize an active site bound Zn²⁺ for catalysis.⁶ In particular, the interaction of CPA with **2**, **3**, and **4** was studied with a view to determining if some degree of specificity might be attainable in the inhibition process.⁷ For comparison, the inhibition of CPA by *o*-phenanthroline (OP), a relatively nonspecific inhibitor known to inhibit CPA by removal of the catalytically essential zinc ion from the active site of the enzyme,⁸ was studied in parallel.

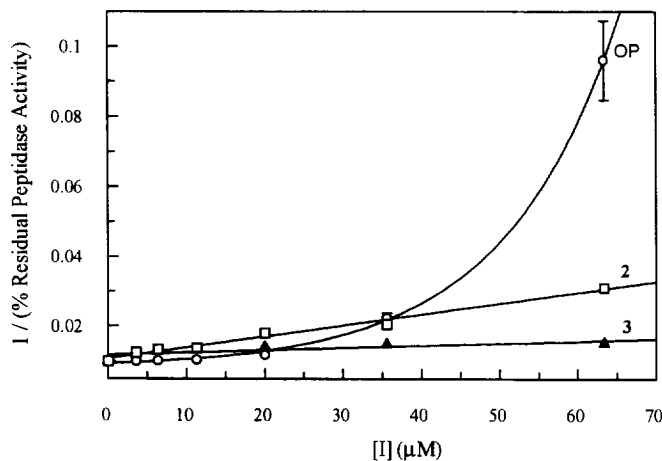
Table 1: Inhibition of CPA and ACE by N-Acylhydrazones

NAH	Inhibition of CPA	Inhibition of ACE
2	IC ₅₀ = 29 μ M	5 % at 63 μ M [†]
3	33 % at 63 μ M [†]	3 % at 63 μ M [†]
4	17 % at 63 μ M [†]	2 % at 63 μ M [†]

Peptidase activity of CPA⁹ was monitored at 265 nm using 0.5 mM HP¹⁰ in 25 mM Tris, 0.5 M NaCl, pH 7.5, containing 3.5% ethanol (v/v), 25 °C, at [CPA] = 200 nM. Peptidase activity of ACE was monitored at 330 nm using 0.1 mM FAPGG¹¹ in 50 mM Hepes, 0.3 M NaCl, pH 7.5, containing 5% DMSO (v/v), 25 °C, at [ACE] = 0.03 units/mL.

[†]Solubility problems precluded the possibility of determining IC₅₀ values for these compounds.

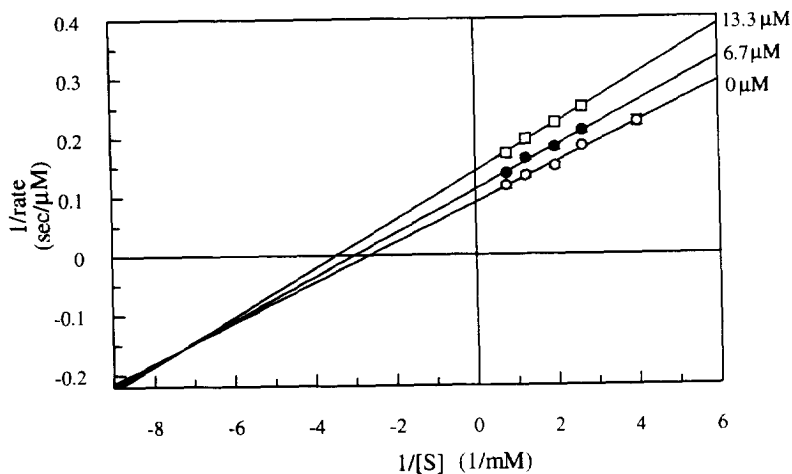
Inhibition of the proteolytic activity of CPA was studied by examining the influence of potential inhibitors on the rate of CPA-catalyzed hydrolysis of hippuryl-L-phenylalanine (HP) as monitored by absorbance changes at 265 nm. As shown in Table 1, the peptidase activity of CPA was found to be susceptible to inhibition by NAH's with **2** (IC₅₀ = 29 μ M) being the most potent of the NAH's studied. That the inhibition process might be associated with interactions of the inhibitors with the active site metal ion is suggested by the observation that **4**, which lacks one of the metal ion binding sites, is a very weak inhibitor. On the other hand the observation that **3**, which is expected to have comparable metal ion affinity to that of **2** since it possesses the same metal ion binding sites but lacks the benzenoid ring fused to the hydroxyl-bearing ring, is a much weaker inhibitor than **2** suggests that interactions with structural features of the active site other than the metal ion play an important role in the inhibition of CPA by NAH's.

Figure 2: Dixon plot of the inhibition of CPA by N-Acylhydrazones:

Peptidase activity was monitored at 265 nm using 0.5 mM HP and 200 nM CPA in 25 mM Tris, 0.5 M NaCl, pH 7.5, containing 3.5% EtOH (v/v), at 25 °C. For the inhibition of CPA by OP, CPA was pre-incubated with OP for 1 hr at 5 °C prior to peptidase activity measurement, as reported by Coombs *et al.*⁸ Preincubation of CPA with **2**, **3** or **4** did not enhance inhibition. The data points are the average of two or more separate determinations. Error bars are shown where the standard error exceeds 6%. For graphical presentation, the OP data were fitted to a single exponential function whereas the data for **2** and **3** were fitted to linear regression.

Analysis of the inhibition kinetic data for **2** and **3** by the Dixon plot method reveals linear relationships typical of simple reversible enzyme inhibition. These observations are in contrast to the nonlinear Dixon plot observed for inhibition by OP (Figure 2), which has been shown to inhibit CPA by removal of the essential metal ion from the enzyme active site.⁸ The apparently parabolic Dixon plot for OP inhibition may result from binding of two molecules of OP, followed by departure of a metal complex incorporating the catalytic zinc ion and two molecules of the inhibitor. The double-reciprocal plot shown in Figure 3 indicates that the inhibition by **2** is not simply competitive. This type of pattern of intersecting lines in the double reciprocal plots is consistent with a mixed inhibition mode, where the inhibitor may bind to the free enzyme (E) and the enzyme-substrate complex (ES).¹²

Figure 3: Double-reciprocal plot of the inhibition of CPA peptidase activity by **2:**

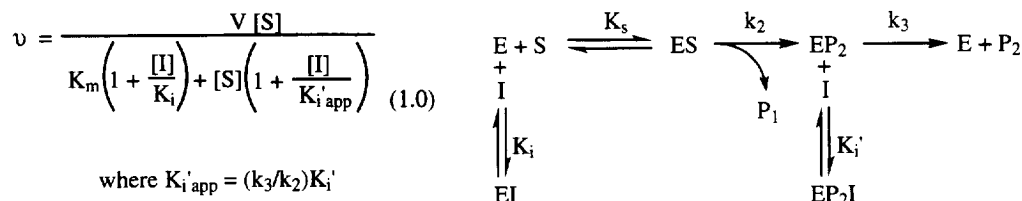


Enzyme assays were carried out using 25 mM Tris, 0.5 M NaCl, pH 7.5, containing 3.5% EtOH (v/v), 25 °C, at [CPA] = 132 nM. HP concentrations were varied from 0.25 mM to 1.3 mM, and **2** concentrations of 0, 6.7, and 13.3 μM were used. Each data point is the average of three or more separate determinations. Standard error bars are smaller than the symbols shown.

To investigate further the mode by which **2** inhibits CPA, molecular modeling studies involving potential modes of binding of **2** to E and ES were carried out.¹³ This study employed an X-ray crystallographic structure of **2**, which is shown in Figure 4 as a stereoscopic framework representation.¹⁴ Attempts to dock **2** into the active site S_1/S_1' -subsite region were unsuccessful due to the size and bulkiness of the inhibitor structure. Furthermore, it was clear that once the substrate HP was bound productively in the active site, there was insufficient free volume remaining in the S_1 and S_2 subsites to allow for the binding of **2**. These observations led us to examine in detail the report of an alternative non-productive binding mode defined in X-ray crystallographic studies. Christianson and Lipscomb¹⁵ found that the slow hydrolyzing substrate, N-benzoyl-phenylalanine, could bind to the enzyme-product complex CPA-Phe such that the hydrolysis product, Phe, occupies the S_1' -subsite, and the substrate, N-benzoyl-phenylalanine, occupies the S_1 and S_2 -subsites. Since Phe is also a hydrolysis product for HP, it occurred to us that **2** might bind to span the S_1 and S_2 subsites in a manner similar to that observed for N-benzoyl-phenylalanine. With Phe present in the S_1' -subsite, this would correspond to an enzyme-product-inhibitor ternary complex, whereas in the absence of Phe such binding

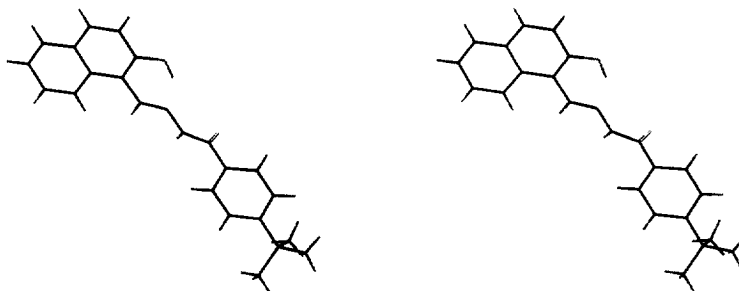
would yield an EI complex with insufficient space available to allow binding of the substrate. The appropriate kinetic model is shown below in Scheme 1 with the derived initial rate expression 1.0.¹⁶ Using nonlinear regression,¹⁷ the data shown in Figure 3 were fitted to equation 1.0, where the K_i was determined to be 47 ± 16 μM , and the apparent K_i' , which, in this model, is related to the true K_i' by the factor k_3/k_2 , was determined to be 28 ± 3 μM . Since k_2 is expected to be less than k_3 for HP hydrolysis,¹⁸ the true $K_i' = (k_2/k_3)K_i'$ should be smaller than the measured K_i' app.

Scheme 1



In order to help deduce a molecular mechanism consistent with this kinetic model of the inhibition process, possible CPA-product-inhibitor complexes were investigated with further modeling studies.¹³ Using Lipscomb's crystallographic study¹⁵ of the binding of N-benzoyl-phenylalanine to the CPA-Phe complex as a guide, the binding of **2** to the CPA-Phe complex was modeled.

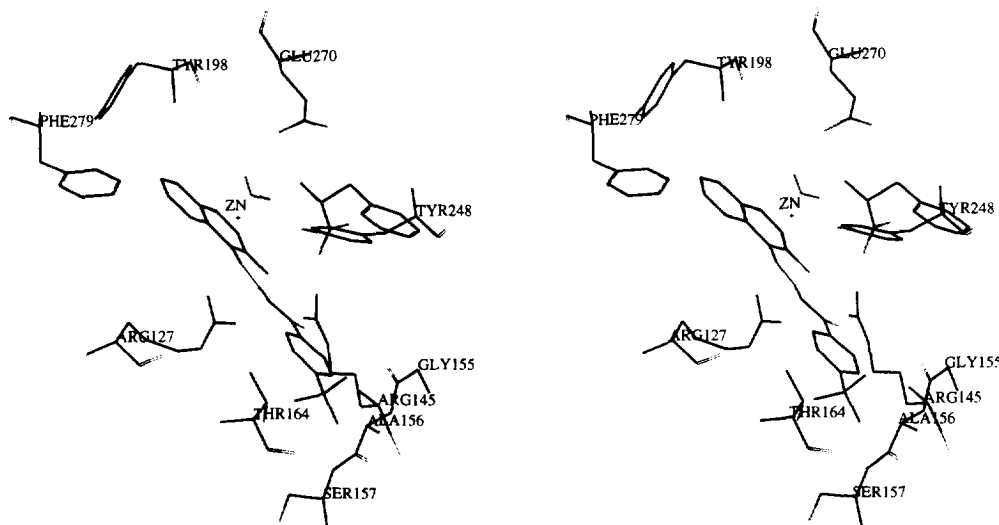
Figure 4: X-ray crystal structure of N-(4-*t*-butylbenzoyl)-2-hydroxy-1-naphthaldehyde hydrazone (2**).**



It was found that direct interactions between the metal binding sites of **2** and the active site zinc ion were strongly disfavoured by steric interactions. As a result, it was decided that inclusion of a water molecule as the fourth zinc ligand would be necessary.¹⁹ Since the pK_a of the hydroxyl group of **2** was determined to be 9.62 ± 0.08 , the unionized form of the phenol was modeled.²⁰ The docking of **2** into the S_1/S_2 region of CPA such as to minimize steric repulsions was followed by a molecular mechanics energy minimization. In the resulting energy minimized structure (Figure 5), **2** is oriented such that the **B** ring of the naphthalene ring is placed into the hydrophobic pocket of the S_1 -subsite formed by the side chains of Tyr-198 and Phe-279. The rest of structure **2** lies in a cleft formed by the active site residues Arg-127, Arg-145, Tyr-248, Gly-155, Ala-156, Ser-157 and Thr-164. The aromatic ring of the *t*-butylbenzoyl group lies within favourable van der Waals distance of Gly-155, Ala-156 and Ser-157. The hydroxyl group of Thr-164 appears to interact with the π -electron cloud on the face of this phenyl group with a distance of 3.68 Å separating the Thr-164 OH and the center of the phenyl ring. The hydroxyl oxygen of **2** interacts with Arg-127 and Arg-145. The carbonyl

oxygen of the amide group of **2** is hydrogen bonded to Arg-145. The Phe component of the ternary complex is bound into the S_1 '-subsite with the same interactions that are observed with the Phe substructure in the CPA-Phe-(N-benzoyl-phenylalanine) complex.¹⁵ There is an additional electrostatic interaction between the NH_3^+ group of Phe and Glu-270. The only interaction observed between the Phe hydrolysis product and **2** is a 2.75 Å interaction between a hydrogen of the NH_3^+ group and the C-3 carbon of the naphthalene ring. This interaction is considered to be electrostatically favourable because of the partial negative charge at C-3 (-0.152 as determined using MOPAC calculations).

Figure 5: Energy minimized complex between CPA, phenylalanine and 2.



These proposed interactions in the ternary complex not only rationalize the affinity **2** for CPA, but also may help explain the lack of binding ability of **3** and **4** to CPA. The NAH **3** lacks the extra phenyl ring found in **2**, which interacts favourably with the hydrophobic pocket of the S_1 -subsite. The NAH **4** lacks the C-2 hydroxyl group which is involved in important interactions with the active site Arg-127 and Arg-145. Another important observation concerning this hypothetical interaction between CPA and **2** is that the hydrolysis product Phe need not be bound to CPA in order for **2** to bind to the S_1/S_2 subsites in this orientation, where the favourable interactions with S_1/S_2 subsites are very similar in the models of the ternary complex (CPA-**2**-Phe) and the binary complex (CPA-**2**). Thus, the binding of **2** to free CPA may be qualitatively very similar to that suggested for the binding of **2** with the CPA-Phe complex.

In conclusion, it has been shown that the NAH **2** is a relatively specific inhibitor of CPA with no activity against ACE. Kinetic and molecular modeling studies suggest that **2** binds to the S_1/S_2 subsites of CPA unlike normal substrates and known competitive inhibitors which interact strongly with the S_1 ' subsite and with the active site metal ion. These results, which indicate that effective inhibition of a metalloprotease can result from the binding of an inhibitor to an enzyme product complex, suggest that such potential binding modes should be considered in the rational design of inhibitors for other metalloproteases.

Acknowledgments: R.S. Fletcher and E.H. Rydberg are thanked for preparing the NAH's used in this study. This research was funded by operating grants from the Canadian Foundation for AIDS Research (CANFAR) (to MAP and GID) and the Natural Sciences and Engineering Research Council of Canada (NSERC) (to GID). The molecular modeling studies were performed on an SGI R4400 Indigo2 computer using Sybyl® (Tripos Associates Inc.) software purchased with funds provided by an NSERC Collaborative Research and Development Grant and by Uniroyal Chemical Ltd. Research Laboratories, Guelph, Ontario.

References and Notes:

1. Baker, E.; Richardson, D.; Grass, S.; Ponka, P. *Hepatology*. **1992**, *15*, 492.
2. Li, R.; Chen, X.; Gong, B.; Selzer, P. M.; Li, Z.; Davidson, E.; Kurzbarn, G.; Miller, R. E.; Nuzum, E. O.; McKerrow, J. H.; Fletterick, R. J.; Gillmor, S. A.; Craik, C. S.; Kuntz, I. D.; Cohen, F. E.; Kenyon, G. L. *Bioorg. Med. Chem.* **1996**, *4*, 1421.
3. Dimmock, J. R.; Baker, G. B.; Taylor, W. G. *Can. J. Pharm. Sci.* **1972**, *7*, 100.
4. (a) Borkow, G.; Fletcher, R.S.; Arion, D.; Dmitrienko, G. I.; Parniak, M. A. *19th Int. Congress Chemother., Montreal 1995*; (b) Borkow, G.; Fletcher, R.S.; Arion, D.; Dmitrienko, G. I.; Parniak, M. A. *Biochemistry* **1997**, *36*, 3179-3185.
5. Spencer, P. C.; Fletcher, R. S.; Dmitrienko, G. I.; Parniak, M. A. *78th Canadian Society for Chemistry Conference and Exhibition*, Guelph, ON, May 1996, Abstract # 1039.
6. (a) Christianson, D. W.; Lipscomb, W. N. *Acc. Chem. Res.* **1989**, *22*, 62; (b) Bünnig, P.; Holmquist, B.; Riordan, J. F. *Biochem. Biophys. Res. Commun.* **1978**, *83*, 1442; (c) Bünnig, P.; Riordan, J. F. *J. Inorg. Biochem.* **1985**, *24*, 183.
7. CPA (bovine, Type I) and ACE (rabbit lung) were purchased from Sigma. The NAH's, **2**, **3**, and **4**, were synthesized by condensing 4-*t*-butylbenzoic acid hydrazide with 2-hydroxy-1-naphthaldehyde, salicylaldehyde and 1-naphthaldehyde respectively using conditions similar to those described by Edward *et al.* (Edward, J.T.; Gauthier, M.; Chubb, F.L.; Ponka, P. *J. Chem. Engin. Data* **1988**, *33*, 538) and were fully characterized by ¹H and ¹³C NMR, mass spectrometry and combustion analysis.
8. Coombs, T. L.; Felber, J.; Vallee, B. L. *Biochemistry* **1962**, *1*, 899.
9. CPA concentration was determined spectrophotometrically using $\epsilon_{280} = 6.42 \times 10^4 \text{ M}^{-1}\text{cm}^{-1}$: Holmquist, B.; Vallee, B. L. *Proc. Natl. Acad. Sci. U.S.A.* **1979**, *76*, 6216.
10. Folk, J. E.; Schirmer, E. W. *J. Biol. Chem.* **1963**, *238*, 3884.
11. Holmquist, B.; Bünnig, P.; Riordan, J. F. *Anal. Biochem.* **1979**, *95*, 540.
12. Segel, I. H. *Enzyme Kinetics*; John Wiley and Sons: New York, 1993; pp 170-178.
13. Molecular modeling studies employed Sybyl 6.2® (Tripos Associates Inc.) on an SGI Indigo2 R4400 XZ graphics work station. Coordinates for the CPA-(Gly-Tyr) complex, from the Brookhaven Protein Data Bank (pdb3cpa.ent, Rees, D. C.; Lipscomb, W. N. *Proc. Natl. Acad. Sci. U.S.A.* **1983**, *80*, 7151), were used to build the CPA-Phe-2 complex. The Gly-Tyr inhibitor was removed and models of Phe and **2** were docked in the active site using Lipscomb's studies of the complex of CPA with Phe-(N-benzoyl-phenylalanine)¹⁵ as a guide. The resulting complex was then minimized using the geometry optimization algorithm MAXIMIN2 (Anneal). For the minimization, the charges were calculated using the Gasteiger-Hückel method (Gasteiger, J.; Marsili, M. *Org. Mag. Res.* **1981**, *15*, 353), and Zn²⁺ was assigned a charge of +2. The minimization involved Phe, **2** and residues within a 15 Å radius around the active site and was conducted until the energy difference between iterations was less than 1 cal/mol.
14. Fletcher, R. S.; Rydberg, E. H.; Taylor, N. J. unpublished results from this laboratory.
15. Christianson, D. W.; Lipscomb, W. N. *J. Am. Chem. Soc.*, **1987**, *109*, 5536.
16. Expression 1.0 was derived using the King-Altman method: King, E. L.; Altman, C. J. *J. Phys. Chem.* **1956**, *60*, 1375.
17. Kinetic data were analyzed using the software package Grafit 3.01® (©Erithacus Software Ltd.)
18. Hydrolysis, rather than product release, is the rate-limiting step for the peptidase activity of CPA: (a) Galdes, A.; Auld, D. S.; Vallee, B. L. *Biochemistry* **1986**, *25*, 646; (b) Geoghegan, K. F.; Galdes, A.; Hanson, G.; Holmquist, B.; Auld, D. S.; Vallee, B. L. *Biochemistry* **1986**, *25*, 4669.
19. X-ray crystallographic studies have shown that, in the absence of a Zn²⁺-binding inhibitor, H₂O is the fourth ligand to the active site Zn²⁺ (where His-69, Glu-72 and His-196 are the other active site ligands): (a) Lipscomb, W. N. *Acc. Chem. Res.* **1970**, *3*, 81; (b) Christianson, D. W.; Lipscomb, W. N. *Proc. Natl. Acad. Sci. U.S.A.* **1986**, *83*, 7568; (c) Lipscomb, W. N.; Sträter, N. *Chem. Rev.* **1996**, *96*, 2375.
20. The pK_a was determined spectrophotometrically (Albert, A.; Sargeant, E. P. *The Determination of Ionization Constants*, 3rd ed; Chapman and Hall: New York, 1984; pp 70 - 101). Molecular modeling with the ionized form of **2** yielded a structure qualitatively very similar to the complex of non-ionized **2** with CPA which is described above.